METRICA
METRology Institutional CAtalog

ISTITUTO NAZIONALE DI RICERCA METROLOGICA
Repository Istituzionale

A New Approach to Measure the Energy On-Board Train During Braking

This is the author's accepted version of the contribution published as:

Original
A New Approach to Measure the Energy On-Board Train During Braking / Delle Femine, A., Signorino, D., Gallo, D., Giordano, D.. - In: IEEE TRANSACTIONS ON INSTRUMENTATION AND MEASUREMENT. - ISSN 0018-9456. - 71:(2022), pp. 1-11. [10.1109/TIM.2022.3165743]

Availability:
This version is available at: 11696/76222 since: 2025-09-19T14:19:57Z

Publisher:
IEEE-INST ELECTRICAL ELECTRONICS ENGINEERS INC

Published
DOI:10.1109/TIM.2022.3165743

Terms of use:

This article is made available under terms and conditions as specified in the corresponding bibliographic description in the repository

Publisher copyright
IEEE
© 20XX IEEE. Personal use of this material is permitted. Permission from IEEE must be obtained for all other uses, in any current or future media, including reprinting/republishing this material for advertising or promotional purposes, creating new collective works, for resale or redistribution to servers or lists, or reuse of any copyrighted component of this work in other works

(Article begins on next page)

16 November 2026

A new approach to measure the energy on-board train during braking

Antonio Delle Femine, *Member, IEEE,* Davide Signorino, *Member, IEEE,* Daniele Gallo, *Member, IEEE,* Domenico Giordano, *Member, IEEE*

***Abstract*—Measuring energy wasted during braking by trains is a non-trivial task because it is performed by power semiconductor devices that switch high current levels at a few hundred hertz. The chopped signals produced are difficult to analyze, not only for the high switching frequency but also for the high slew rate that produces even higher harmonic content. In this harsh scenario, it is challenging to guarantee an adequate level of accuracy and it could be very expensive for railway operators, who often completely renounce measuring these quantities of interest, estimating it from mechanical quantities. In a previous paper, the authors have already faced this issue by developing an accurate technique usable offline. Here, two simplified methods with suitable accuracy levels for train energy management, and easy to be implemented on train control unit are proposed. The paper describes the phenomena of interest and related measurement issues. A numerical solution together with a deep analysis on the input quantities needed are presented. The methods are applied to experimental data from a measurement campaign, conducted on-board train in the northern part of Italy. Furthermore, the metrological performances of the methods are assessed by adopting as reference the off-line technique.**

***Index Terms*—Power and Energy measurement, Railway system, Dynamic Braking, Braking Rheostat, Wasted Energy, Chopped Waveforms, Power Electronics.**

I. Introduction

THE efficiency of the European railway system is one of the aims declared in the white paper for efficient transport system [1]. As it is known, the DC railway systems, which represent about 35% of the European electrified railway lines, are unidirectional, which means that the energy generated because of the dynamic braking of the trains cannot be delivered to the upstream AC network. The energy generated by electric braking is dissipated by braking rheostats, placed on-board trains, and thus wasted [2]. The importance of dynamic braking and the descriptions of regenerative and dissipative braking are discussed in [3]. The scientific and technical world pays great attention to the new solutions that allow the saving of such energy. Several technical solutions are proposed: reversible substations that inject the energy to the upstream AC grids for suburban [4], or railway [5], storage systems on-board [6], and/or in substation [7], able to collect and store the braking energy, and algorithms for the identification of the optimal speed profile [8], and algorithms for the cooperation among braking and absorbing of multiple trains [9]. Most of these activities are based on simulation, which do not represent the actual variability of real cases. The actual energy dissipated depends not only on braking effort and time duration but also on the driving style, the traffic conditions, the catenary resistance, and even on the difference between the supply voltage amplitude and the threshold voltage that triggers the insertion of the braking rheostat [10]. Because of the high variability of such influence quantities, it is very important to collect field data associated with all the actual operating conditions of the system. Such information is valuable for the designers aimed at improving the energy efficiency of the whole railway system.

On-board trains, there are often measurement systems already installed, commonly used for diagnostic or control purpose, but these are not suitable for fully analysing all energy flows. In fact, the commonly used instrumentation does not acquire all the electrical quantities needed and it works with a sampling frequency of few tens of hertz, that is not enough for the dynamic of involved signals. In [11] the problems of measuring pulsed voltage and pulsed current are exposed, which increase the cost of the necessary equipment. Measuring dissipated energy with an adequate level of accuracy is too expensive for railway operators who often refrain from measurement and prefer estimation based on mechanical quantities, affected by high uncertainty.

A cost-effective solution to measure energy dissipated on board with an adequate level of accuracy is needed. But, at the time of writing, to the best authors' knowledge, no article specifically addresses these energy measurement needs. The author faced this measurement issue in [12], proposing a high accuracy offline technique. It is based on the determination of the correction coefficient that allows compensating for the frequency response of the transducer and the presence of stray inductance. The present paper proposes a technique to exploit already installed measurement systems and other information available to the train control system to quantify the energy wasted during braking correctly; the technique reveals easy to implement for already operating traction units. This new finding consists of neglecting two specific measurement issues, successively correcting the approximated result with a numerically determined function; this last reveals to be constant in most cases.

The activities on the reliability assessment of the proposed method and statistical analyses on the input quantities have been carried out thanks to the huge amount of data provided by the European Project 16ENG04 MyRailS [13]. Long measurement campaigns carried out on-board the DC 3 kV E464 locomotive, widely used for commuter transport,

D. Gallo and A. Delle Femine were at Università della Campania: Luigi Vanvitelli, Aversa, Italy, e-mail:daniele.gallo@unicampania.it

D. Giordano and D. Signorino were at the Italian National Metrological Institute (INRiM), Torino, Italy, e-mail:d.giordano@inrim.it

has been performed [14]. This activity has been carried out in collaboration with Trenitalia, the most important Italian railway company. The reliability of the method has been investigated by performing a comparison with the rigorous approach for the braking energy estimation proposed in [12].

The paper is organized as follows: sect. II provides an overview of the energy flow during dynamic braking. Sect. III focuses on the measurement issues in the determination of the wasted braking energy. The proposed measurement approach for the determination of this energy is provided in sect. IV. Sect. V describes in detail the measurement setup and the campaign carried out on-board the E464 with reference to the power/energy dissipated by the braking rheostat. Sect. VI describe with example the energy exchange phenomena between the pantograph and the line during dynamic braking. Sect. VII hosts the analysis of the data acquired in field, in order to clarify the application on real measurement and define the variability of the input quantity model. Finally, sect. VIII provides a comparison between the reference and the proposed method for the wasted energy determination applied to some example routes.

II. Energy Flow during Dynamic Braking

As well known, one of the main advantages of using electric motors with respect to combustion engines lies in the implementation of dynamic braking. The latter is a mechanism that allows using the traction motor as a brake, avoiding or reducing the traditional mechanical braking that is more expensive in terms of maintenance needs. During dynamic braking, the traction inverters reduce the operating frequency, thus reducing the motor speed. In this condition, the motor acts as a generator opposing resistive torque to the spin. Moreover, the generated current flows back to the DC side through the reverse polarity protection diodes. This solution allows converting kinetic energy back to the electric form so that it could be completely or partially delivered, through the input filter, to the upstream supply system.

Currently, the DC supply system of a railway network is obtained by the AC 50 Hz through the six or twelve pulses passive rectifier. This kind of energy converter is unidirectional, i.e. it blocks the energy flow towards the mains. This configuration imposes that the balance between generator and loads must be found within the DC system, therefore, the energy recovered during braking can only be used by other trains on the line. Actually, the injection of energy on the catenary during regenerative braking always produces an increment of voltages whose amplitude depends on the availability of the loads that can absorb the recovered energy and their distance from the braking train. When loads are too far or absent, the train dissipates the energy on-board.

Fig. 1 models a section of the DC system consisting of one ESS (Electrical Sub-Station), which feeds a double track line. Two trains are present on the line: one is accelerating, leaving the station, with absorption of current; the other one, placed on the other track, is approaching the station, thus it is braking, with a generation of current. The transfer of power between the two trains entails a voltage increase to overcome

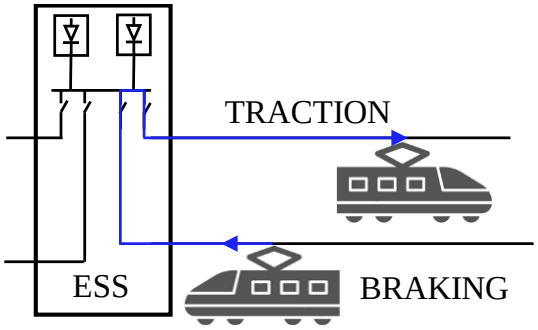


Fig. 1. Energy exchange between two trains on the same section of line.

the drop across the portion of line from the braking train to the train in traction. So the higher is the power, the higher must be the required voltage increase. Of course, the voltage cannot rise indefinitely for safety reasons [15]. Thus when voltage exceeds a certain threshold, on-board dissipation is activated, limiting power injection. Specifically for the Italian Railway System only at voltages lower than 3.8 kV, the energy may be completely sent back to the catenary; over this value the on-board dissipation is activated to limit the voltage increment. In detail, when the voltage line reaches a value between 3.8 kV and 3.9 kV, a mix of dissipative and regenerative braking is implemented. Above 3.9 kV, purely dissipative braking is applied. The lack of storage systems or reversible substations, in most Italian railway systems, limits the possibility of recovering the braking energy and, consequently, the energy efficiency of the system.

To clarify how dissipation is implemented, it is worth examining an electrical diagram of the input stage of a typical locomotive. The train on which this research was carried out is the E464 (rated power of 3.5 MW and a maximum speed of 160 km/h). It is owned by Trenitalia and used for commuter transport. A simplified circuital model of the input stage of this locomotive is illustrated in Fig. 2. The traction system is composed of four asynchronous three-phase motors that are supplied by two inverters, series-connected, with a rated voltage of 1.5 kV each. A capacitor C_F of 17.1 mF is placed in parallel to each inverter. The two capacitors, together

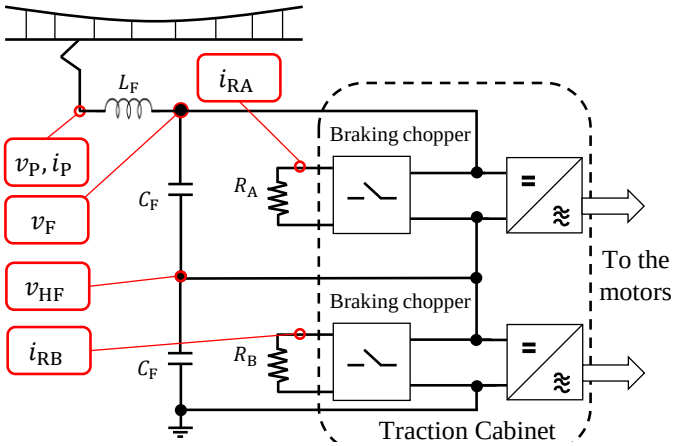


Fig. 2. E464 input stage drawing with quantities of interest.

with the inductor L_F of 8.5 mH, constitute the input stage filter whose purpose is to limit the disturbance between the supply line and the locomotive. Moreover, a chopper circuit is present, which can be considered a controllable switch, able to feed the braking rheostat bank when necessary. The braking chopper, controlling the duty cycle of the PWM (Pulse Width Modulation), regulates the amount of power to be dissipated on the braking rheostats, depending on the share of energy that can be recovered at that moment. In this way, when voltage exceeds prescribed limits, the surplus of energy can be partially or totally dissipated on the rheostats: the higher is the voltage, the higher is the duty-cycle of the chopper.

III. The Measurement of Dissipated Energy issue

In order to study the time behaviour of involved signals and problems concerning the measurement of dissipated energy, a simplified model that represents the circuit of the braking chopper is presented in Fig. 3. This circuit switches on and off the GTO (Gate Turn Off thyristor) at the frequency of the chopper. The braking rheostats were modelled with a series between resistor and inductor, where the latter takes into account the stray inductance of the braking rheostats [12]. A simulation of the circuit of Fig. 3 was performed. The values adopted for the RL circuit model are $R = 1.505\ \Omega$, $L = 12\ \mu$H, and $T = 1/260$ s, which are the nominal values for the E464 locomotive, the case study of the present research. Table I summarizes the main characteristics of the braking rheostats of the E464, as reported in [16].

The step response, obtained by choosing $\delta = 3\%$, is shown in Fig. 4. Note that the voltage drop across the GTO can be considered negligible only when the thyristor is turned on. For this reason the voltage v_δ across R and L is equal to v_{INV} only when switch is closed. Instead, when the GTO is turned off, the inductance discharge accumulated energy over the resistance, the voltage goes near to zero (to be precise, it goes down to the forward voltage drop of the diode), simultaneously the rheostat current does not become zero instantly.

Measuring the power dissipated on the braking rheostats is a challenging and very difficult task for two main reasons. The first reason is that the signals of interest have pulsed waveform with high frequency content due to high slew rate together with high chopper frequency. The sampling frequency currently used in railway applications is not suitable for acquiring such a signal. Moreover, the measurement requires the adoption of expensive large bandwidth transducers not employed in the railway sector. The situation is even worst for a very low duty-cycle. To give an idea of what actually happens with braking

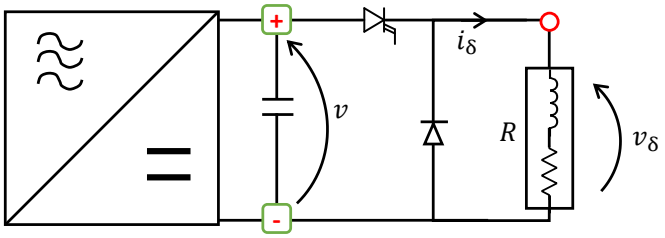


Fig. 3. Electrical drawing of the braking chopper system

TABLE I
Braking Rheostats Characteristics

Parameter	Value
Maximum power	2 x 1200 kW
Resistance at 20 °C	2 x 1.52 Ω
Maximum resistance variation in range [20 600] °C	5%
Operating voltage	1500 kV
Maximum RMS current	900 A
Stray inductance	12 μH

rheostats, in the case of study of this research, a typical current pulse with a duty of 3% at the chopper frequency of 260 Hz, is characterized by a high current level of 1200 A that lasts only 115 μs.

The second reason is that voltage and current cannot be measured at the same electrical node. In fact, the terminals of the rheostats downstream the chopper, where the pulsed current can be measured and the current probe is placed, are covered with unmovable insulations. For this reason, the voltage probe can only be placed upstream the chopper, where the voltage is constant (not pulsed). The measurement points are marked in green for the voltage and red for the current in Fig. 3. Therefore, the product of the inverter voltage v and the rheostat current i_δ is not the actual power dissipated by the braking resistor but is an overestimate. As it can be seen from Fig. 4, the overestimation of dissipated power ($v \cdot i_\delta$) is due to the decay trend of current, evidenced in red ($i_{\delta \mathrm{F}}$), wrongly included in the power computation. This happens because the voltage at the measuring point is constant and not pulsed, unlike v_δ. The overestimation of pulse energy becomes significant, especially for low duty-cycle values.

IV. Methodology for the estimation of the braking rheostat energy

In [12], an offline technique to correctly take into account the inductance transient was presented, which allowed estimating, with good accuracy, the energy dissipated by the braking rheostats, starting from the voltage and the current measured

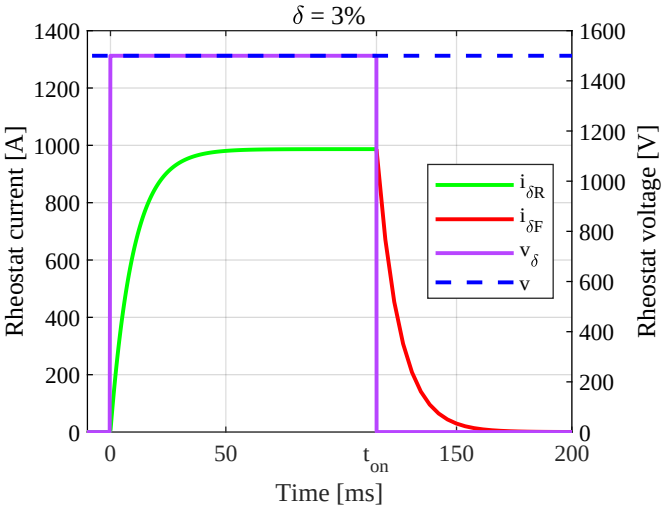


Fig. 4. Current response to voltage pulse in the RL circuit

according to Fig. 3. This paper proposes an alternative online method for estimation of such energy that can be used directly on board the train, more accurate than those currently implemented by railway operators.

To identify a way that allows simple calculations and the use of quantities already available or easily measurable, it is possible to intentionally neglect the charge and discharge transient of the inductance. By ohm's law, an approximated estimation, E_{a}, of dissipated energy, can be calculated as:

$$E_{\mathrm{a}} = \int_0^T \frac{v(t)^2}{R}\, dt \approx \int_0^{t_{\mathrm{on}}} \frac{V^2}{R}\, dt + \int_{t_{\mathrm{on}}}^T 0\, dt = \frac{V^2}{R}\int_0^{t_{\mathrm{on}}} dt = \frac{V^2}{R}\cdot\delta\cdot T \tag{1}$$

where T is the period of the square wave applied to the rheostat, R is the rheostat resistance, V is the amplitude of the high level of v_δ, t_{on} is the time in which the GTO is on, and $\delta = t_{\mathrm{on}}/T$ is the duty-cycle. Note that V can be considered equal to the measured quantities v neglecting the voltage drop across GTO.

This approach is extremely simplified with respect to the nature of the signals analysed, since the voltage is considered constant for the entire pulse period and it completely excludes the presence of the inductance, which does not allow the current to follow the behaviour of the voltage instantaneously. The presence of inductance reduces the energy dissipated by the single pulse (see Fig. 4), reducing the effectiveness of the duty cycle like it is slightly lower than the actual one. So it is possible to define an equivalent square pulse with a slightly lower duty cycle that dissipates the same energy as the real pulse. This can be expressed by introducing a positive quantity ξ to be subtracted from δ in the approximated eq.1 obtaining:

$$E(\delta) = \frac{V^2}{R}\cdot(\delta-\xi)\cdot T \tag{2}$$

Knowing that the real pulse reference energy can be expressed as:

$$E_{\mathrm{REF}}(\delta) = \int_0^T v_\delta(t)\cdot i_\delta(t)\, dt \tag{3}$$

By equating eq.2 to eq.3 it is possible to quantify ξ:

$$\frac{V^2}{R}\cdot(\delta-\xi(\delta))\cdot T = E_{\mathrm{REF}}(\delta) \tag{4}$$

where ξ is a quantity to be subtracted to δ in order to compensate overestimation and to equal the reference energy. ξ can be derived from (4) as:

$$\xi(\delta) = \delta - \frac{E_{\mathrm{REF}}(\delta)\cdot R}{V^2\cdot T} \tag{5}$$

of course ξ is a function of δ. It is possible to evaluate E_{REF} numerically from the circuital simulation described in section III, in discrete form:

$$E_{\mathrm{REF}}(\delta) = \sum_{\mathrm{k}=1}^{N} v_\delta[k]\cdot i_\delta[k]\cdot t_{\mathrm{s}} \tag{6}$$

where t_{s} the simulation time-step and, N is the number of points in a period, note that the dependency from δ is implicit

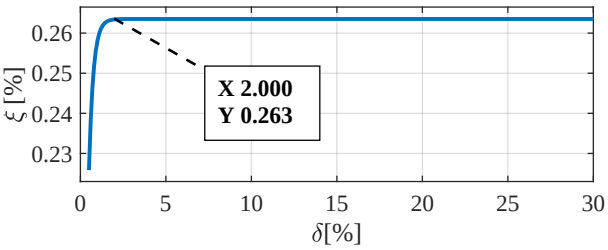


Fig. 5. ξ variability over δ

in $v_\delta[k]$ and $i_\delta[k]$. Using (6) in (5) ξ has been numerically evaluated, its behaviour with respect to delta is shown in Fig. 5. As it can be seen, for $\delta \geq 2\%$, ξ is practically constant, it can be assumed independent from δ and equal to its asymptotic value ξ^*:

$$\xi(\delta) \approx \xi^*. \tag{7}$$

The proposed method can be synthesized as:

$$E(\delta) = \frac{V^2}{R}\cdot(\delta-\xi^*)\cdot T \tag{8}$$

where ξ^* is the constant asymptotic value, in the specific case 0.263%.

To evaluate the performance of the proposed method, the error has been calculated as:

$$\epsilon(\delta) = 100\cdot\frac{E(\delta)-E_{\mathrm{REF}}(\delta)}{E_{\mathrm{REF}}(\delta)} \tag{9}$$

(9) was evaluated by varying δ from 0.5% to 30%, with a 0.1% step. The results are depicted in Fig. 6 in red with $\xi = \xi^*$ and in blue with $\xi = 0$. The blue curve represents the error made, completely neglecting inductance transient; it reveals to be unacceptably high for a wide range of δ. The red curve shows that the proposed method, still maintaining the simplicity of implementation, allows compensating for the error, reducing it practically to 0 for $\delta > 2\%$.

It is important to highlight that the proposed method (8) is very simple to implement, it bypass the problem of measurement point (mentioned in sec. III), because it rely only on the

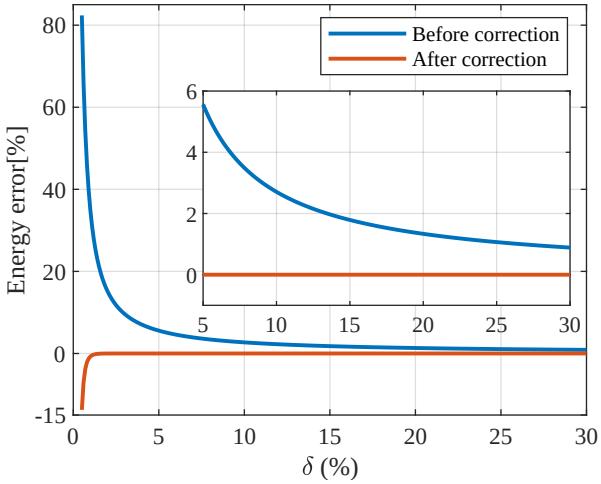


Fig. 6. Energy measurement error before and after the correction though ξ

measurement of the inverter voltage (v). In fact, the duty cycle is a quantity known, usually imposed by the chopper control circuit, and R can be considered constant for the required level of accuracy. The cost-effectiveness of the method is very high, it doesn't require expensive large bandwidth transducers because it does not require the measurement of pulsed signals. Moreover, the inverter voltage measurement is often already implemented in the train control unit, reducing its implementation to a matter of software.

For the best accuracy of the proposed method, it is necessary to know the value of R by characterizing the braking resistor, the obtained value must be first used in the simulation to get an accurate value of ξ^*, then must be used in (8).

A. Insertion of current sensors: an improvement to the method

An aspect that limits the accuracy of the proposed method is that the chopper current can heat the braking rheostats by the Joule effect, and the resistance of the rheostat R varies with temperature [17]. Up to this point, R has been considered constant, but to achieve better performances, the variation of R must be taken into account, measuring currents. To the best authors' knowledge, current measurements are not implemented by the train management systems. Moreover, as mentioned before, the measurement of the chopper current is not a trivial task. In fact those currents have sharp edges and high frequency contents with simultaneously high levels of amplitude. This implies the adoption of expensive high performance current probes and even more expensive digitizer with sufficiently high sample rate. Instead, it is possible to identify a single sample per pulse that represent an estimation of the average current during the pulse itself. This can be achieved by adopting a low-cost analog peak detector, with a step response tuned on the time behaviour of the chopper signal, taking only one sample per chopper pulse. The chopper control circuit can trigger sampling after an opportune delay following the switch activation.

Defining the measured peak current as:

$$\hat{I} = V/R \tag{10}$$

and using this quantity in the eq.8, a new formula for pulse energy evaluation is obtained:

$$E(\delta) = \frac{V^2}{R} \cdot (\delta - \xi^*) \cdot T = V \cdot \hat{I} \cdot (\delta - \xi^*) \cdot T \tag{11}$$

With this approach, the variations in the resistance value are taken into account because are reflected in the variations of $\hat{I}$

V. Measurement Campaign

As mentioned before, to accurately estimate the energy flows during braking in real conditions, an extensive measurement campaign has been carried out on-board the E464 locomotive during its normal commercial service.

With reference to the simplified circuital model of the locomotive input stage illustrated in Fig. 2, the quantities monitored during measurement campaign are depicted with red labels: v_{P} is the voltage at pantograph, v_{F} is the filtered voltage at the input of inverters, v_{HF} is the voltage between the two traction inverters, series-connected, i_{P} is the total current absorbed by the locomotive and i_{RA} and i_{RB} are the pulsed currents that flow through the braking rheostats R_{A} and R_{B}

A. Measurement setup

In order to acquire experimental data on actual energy flows on-board trains, a specific measurement system able to acquire signals with high frequency content was designed, implemented, tested, and installed on an E464 locomotive. The system has been realized by adopting a National Instruments Compact Rio 9034. It is a stand-alone reconfigurable embedded chassis with an integrated real-time controller and, thanks to its reduced size, it could be positioned on the train. The system has been equipped with two NI 9223 voltage acquisition modules with 16-bit resolution, maximum voltage input 10 V, 50 kHz sampling rate, 4 channels each, and synchronized sampling among all 8 channels were used. Furthermore, the GPS module NI 9469, capable of providing a Pulse Per Second (PPS) with an accuracy of 100 ns has been used for time synchronization.

With reference in Fig.2, as transducers for the measurements of v_{P}, v_{F}, and v_{HF}, ULTRAVOLT TF-Series 40 kV resistive-capacitive voltage divider were used. The ULTRAVOLT transducers are designed to make accurate high voltage in-line measurements in DC system, the measurement of ripple on DC with a bandwidth up to 10 MHz.

For i_{P} (see Fig.2), the LEM HOP 2000 transducer was used. The primary nominal rms current of this Hall Effect based transducer is 2000 A, with an output voltage of 4 V. The rated accuracy is not so high (2%), but this transducer was chosen for its dynamic and the possibility of inserting the probe without interrupting the power circuit. Furthermore, the laboratory calibration performed at INRiM allows for compensating systematic error. Some details on the transducer calibration and uncertainty analysis will clarify this aspect in the following.

In order to measure the power dissipated by braking rheostats, two Rogowski coils, designed and realized at INRiM, were used for i_{RA} and i_{RB} [18].

B. Transducers Calibration

All the transducers used in the campaign have been calibrated at Italian National Metrology Institute (INRiM) laboratories under controlled environmental conditions (temperature of 23 $\pm$ 1 °C and the humidity in the [40 60] % range). All the voltage transducers and the transducer used for the current at pantograph have been characterized adopting DC national standards as reference. Instead, the performances of Rogowski coils have been tested using AC 50 Hz national standard; further test has been conducted also at 260 Hz, that is the braking chopper frequency.

As regards the three dividers, five steps in amplitude between 1 kV and 5 kV were performed; for each step, 31 iterations were implemented as prescribed by [19] in order to evaluate repeatability and stability correctly; finally, the type B uncertainty of the reference system (3 $\mu V/V$) was combined too. The transducers showed good amplitude linearity. In fact,

the scale factor variability on the five different amplitudes is kept limited within the uncertainty (140 $\mu V/V$) interval; in other words, the measurement results at the different amplitude levels are compatible. For this reason, the scale factor can be considered constant with the amplitude in the range of interest.

Results coming from the calibration of the HOP 2000 current transducers are shown in Fig. 7. Twenty-four steps in amplitude, in the range -2 kA to 2 kA, with an analysis time of 1 s were performed. The technique adopted is explained in [20]. For each step, 31 iterations were implemented [19] in order to evaluate type A uncertainty correctly. The type B uncertainty for DC current setup is 150 $\mu A/A$ and was combined too. This sensor presents a linearity problem; in fact, it can be noted that the value of the scale factor (SF) significantly changes with the amplitude of the current. Thus the value of the SF can be written as a function of the transducer output voltage, $SF(v_{\mathrm{HOP}})$. In order to use a single SF value, and to estimate the impact of this linearity issue, a statistical analysis has been conducted, using all the v_{HOP} values coming from the measurement campaign averaged over 1 s. It can be assumed that SF is a random variable with the pdf (probability density function) shown in Fig. 8. The mean of the distribution can be used for all subsequent analyses to minimize the linearity issue impact on uncertainty. Moreover, it is possible to adopt the CoV (Coefficient of Variation) as a good estimation of the standard relative uncertainty contribution due to the non-linearity of the current measurements. In fact, according to the GUM Supplement 1 [21] the distributions of the input sources of uncertainty propagates through the model to provide the distribution of the output. Thus being $i_{\mathrm{P}} = SF \cdot v_{\mathrm{HOP}}$, and neglecting the contribution due to the voltage channel, the relative standard uncertainty on the current measurements coincides with that of the SF. Moreover from the cdf (cumulative distribution function) it is possible to easily evaluate also the confidence level of such uncertainty for the real measurements distribution (more than 92 % of the occurrence fall inside the interval 485.76 ± 0.5 %). Laboratory calibration was also performed for the Rogowski coils; the results are shown in Fig. 9. The error bars represent

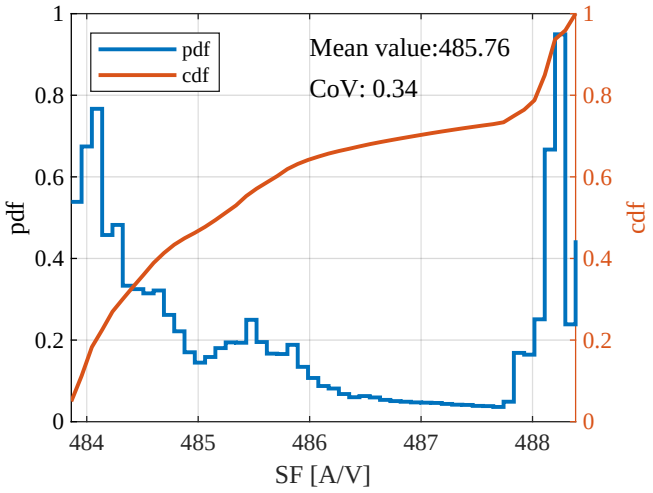


Fig. 8. probability density function of SF

the expanded combined uncertainty at a confidence level of 95.45% (k = 2). As it can be seen, like the voltage dividers, the Rogowski exhibits a minimal variation of scale factor with amplitude. It can be considered almost constant in the range of interest, and the variation with amplitude was included in the uncertainty computation. Of course all active transducers have an offset, that has been opportunely compensated. Moreover experiments in laboratory has been conducted to take into account the temperature as influence factor. The variation of offset and gain with temperature was considered as source of uncertainty. It has been checked that the uncertainty contribution due to temperature variation in the range of measurement campaign maintains lower than the other sources, especially for hop. For sake of brevity, not all the results coming from calibration of transducers, varying the amplitude and the temperature are reported. Table II summarizes the scale factor of each transducer adopted together with expanded combined uncertainty, with a confidence level of 95.45%($k = 2$).

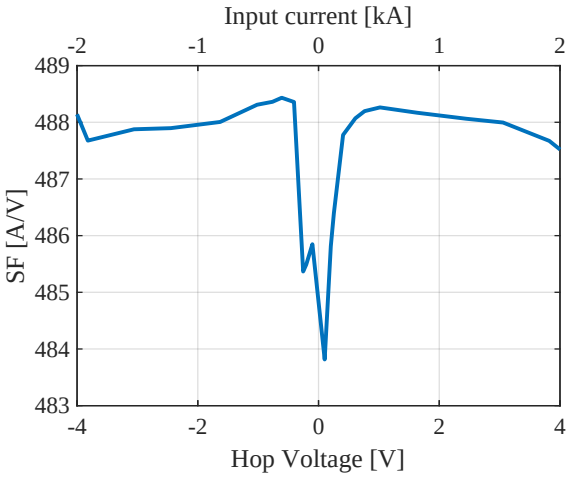


Fig. 7. Scale factor characterization of the LEM HOP 2000 transducer

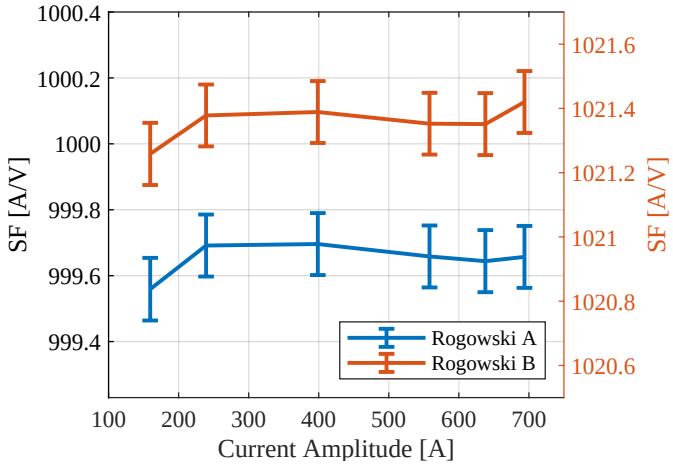


Fig. 9. Scale factor of Rogowski coil with expanded uncertainty ($k = 2$)

TABLE II
SENSORS CHARACTERISTICS

Signal	Scale Factor	U/M	Expanded Uncertainty in DC (k=2)
v_{P}	1016.54569	[V/V]	0.014%
v_{F}	1016.85997	[V/V]	0.014%
v_{HF}	997.58296	[V/V]	0.014%
i_{P}	488.633	[A/V]	0.5%
i_{RA}	999.6509	[A/V]	0.03%
i_{RB}	1021.3581	[A/V]	0.03%

VI. Energy Exchange During Braking

This section shows some data from the measurement campaign that allow a better understanding of the energy exchange phenomena between the pantograph and the line during dynamic braking. The subsequent graphs show the instantaneous powers, calculated as follows:

$$p_{\mathrm{P}}(t) = v_{\mathrm{P}}(t) \cdot i_{\mathrm{P}}(t) \tag{12}$$

$$p_{\mathrm{R}}(t) = (v_{\mathrm{F}}(t) - v_{\mathrm{HF}}(t)) \cdot i_{\mathrm{R1}}(t) + v_{\mathrm{HF}}(t) \cdot i_{\mathrm{R2}}(t) \tag{13}$$

$$p_{\mathrm{T}}(t) = p_{\mathrm{P}}(t) - p_{\mathrm{R}}(t) \tag{14}$$

where all the quantities were defined in section V-A.

Fig. 10a reports the behavior of the line voltage, the power absorption, and the power of rheostats in typical braking. All the quantities in (12), (13), (14) are averaged over 100 ms.

The dashed blue line, V_{TH}, points out the voltage threshold for chopper activation. The braking starts as regenerative, it can be deduced by the negative value of the absorbed power p_{P}, so the power is totally transferred to the line, but the voltage v_{F} starts to increase. Slightly after second 2, the threshold value of 3.8 kV, V_{TH}, is reached, the chopper starts working ($p_{\mathrm{R}} > 0$), and the locomotive wastes part of the power provided by the inverters, p_{T}, on the braking rheostats, the dissipated share start rising, reaching a maximum of 1 MW around second 5 (this is appreciable observing the black line p_{R}). At the same moment (second 5) the braking power is almost 3 MW, consequently the power injected on the line is almost 2 MW. The braking continues in a mixed scenario, between dissipation and generation; when voltage drops under the threshold, the power is totally injected; when the braking effort increases at the second 14 (causing an increment of the line voltage, of course) the dissipation increases in turn.

As previously described, the chopper regulates the amount of dissipated power, varying the duty cycle. This modulation is appreciable in the enlargement reported in Fig. 10b and 10c. Note that, around the second 5, the dissipation is high; in fact, the duty cycle is about 20% (Fig. 10b). In contrast duty cycle is only 4% (Fig. 10c) around the second 10, in which the pantograph voltage drops below the V_{TH} threshold, the power dissipated on the rheostats is minimal and, consequently, the power generated by the traction inverters it is almost totally injected on the line. An example of purely dissipative braking is in contrast shown in Fig. 11. As soon as the braking starts, the voltage reaches the threshold value and the chopper is activated, all the power generated by the traction inverters, p_{T}, is delivered to the braking rheostats for being dissipated. In fact, as it can be clearly seen in figure, the p_{T} is symmetrical to the p_{R} with respect to the time axis, and their sum p_{P} is zero. During this braking, starting from second 6, the inverters provide a power of about 1.3 MW for about 8 seconds that could potentially be reused by other services instead of being wasted.

VII. Application of the Simplified Energy Estimation Methods to Real Test Cases

In order to apply the proposed methods to real test cases from the aforementioned measurement campaign, the input quantities for (8) and (11) must be estimated. The authors has no access to train control unit data and not all the quantities are directly available from measurement data. In particular, only a voltage was measured directly, duty cycle and resistance

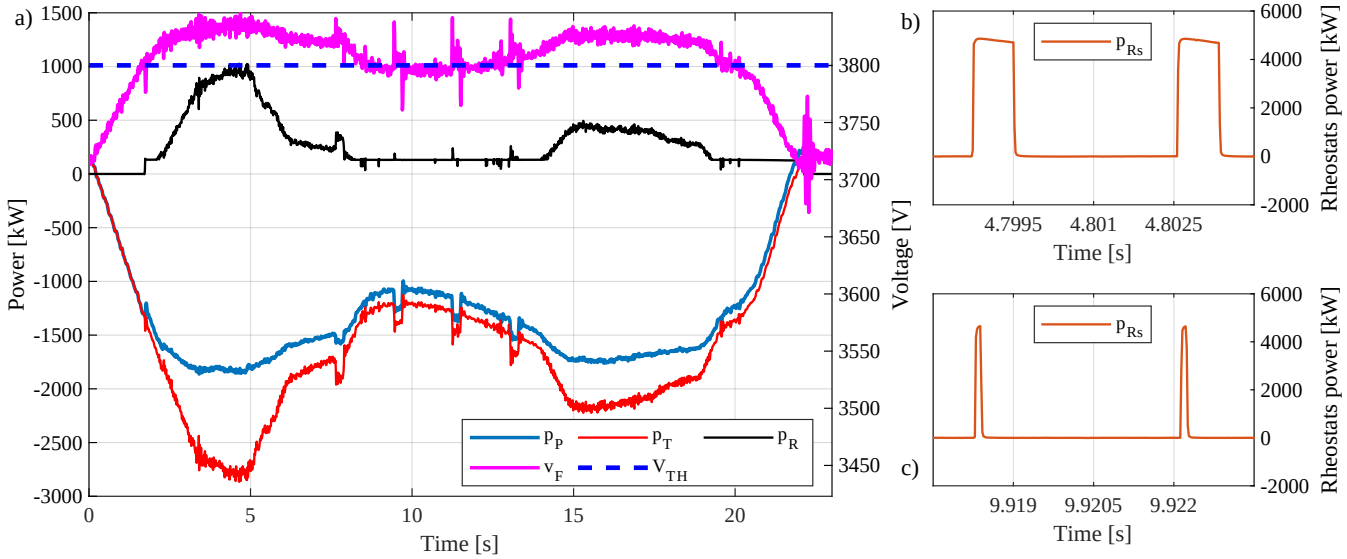


Fig. 10. Example of a mixed braking during Susa - Torino: (a) the powers averaged over 100ms, (b, c) instantaneous rheostats power

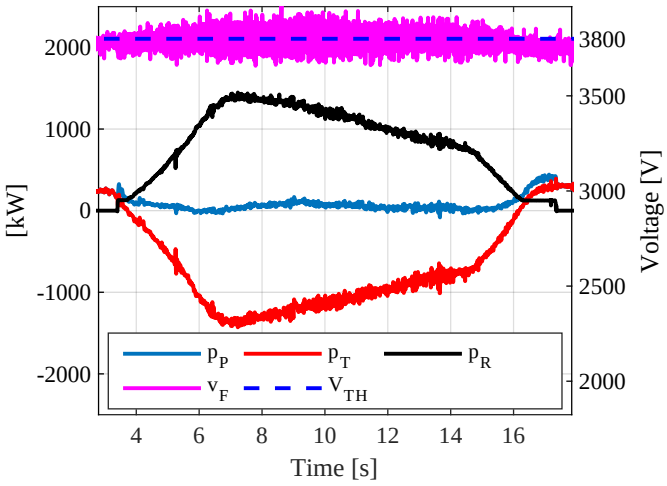


Fig. 11. Example of a dissipative braking during Novara - Domodossola

are derived. In the following the calculation for each input parameter is explained in detail. Furthermore, statistics of the values obtained allow to evaluate the variability of the input quantities.

A. Inverters voltages measurements

The v_{F} and v_{HF} are measured directly as explained in section V-A. Analyzing the rheostats currents i_{RA} and i_{RB}, it has been possible to identify all the chopper pulses over all the measurement campaign. A total of 7'866'069 pulses were collected and analyzed. For each pulses the average value of v_{F} and $v_{\mathrm{F}} - v_{\mathrm{HF}}$ has been determined. In Fig. 12 are depicted the PDF (Probability Density Function) of these two quantities as results of the conducted statistical analyses. As it can be seen from the figure, the two distributions are very close, with a little difference in the mean value. The variability of the voltages of the rheostats is due to the variability of the line voltage, which is divided almost equally on the two inverters. As shown, the average value coincides with half of the chopper intervention threshold; moreover, voltage never overcomes 1950 V, in fact, as stated before, above 3.9 kV, purely dissipative braking is applied to avoid further voltage increase.

B. Duty-cycle estimation

As mentioned before, the duty cycle should be known because it is imposed by the chopper. Unfortunately, this information was not available to the authors of this research. For this reason, it has been necessary to develop a technique to estimate the duty cycle.

A known duty cycle δ has been imposed to the same RL model of section IV. The duty cycle has been estimated on the simulated signal, applying the Matlab $midcross$ function. The obtained result obviously slightly differs from the imposed δ. Varying imposed δ in the range of interest, i.e. from 0.5% to 45%, with a 0.1% step, a set of results has been obtained. Then, adopting a curve fitting tool, an interpolation function has been obtained:

$$\delta = f(\delta_s) \tag{15}$$

where δ_s is the value of the duty-cycle estimated with the $midcross$ method. Then, it has been possible to apply $midcross$ interval estimation and successive curve fitting compensation (15) on the real measurement data for each chopper pulse. In Fig. 13 the PDF and the CDF (Cumulative Distribution Function) of the obtained results are reported. As it can be noted the duty never goes under 2%. This makes the assumption (7) always valid for the case of study. ξ is a constant amount equal to ξ^*, and the error due to this assumption is always 0.

C. Estimation of rheostats resistance and current

For the application of (8) it is essential to accurately know the resistance value of both the rheostats. For the (11) instead an estimation of $\hat{I}$ is needed.

The rated values of resistance for the considered locomotive are declared for 1.52 Ω with an accuracy of ± 5% in all operating conditions (see Table I). Since it is not possible to

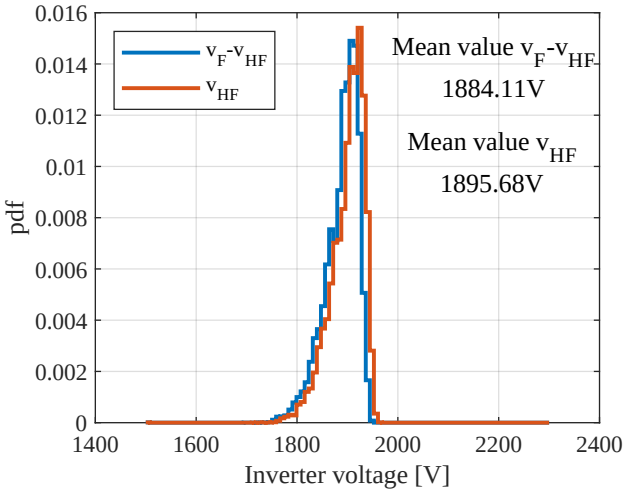


Fig. 12. Statistical analyses of the voltages applied to the inverters.

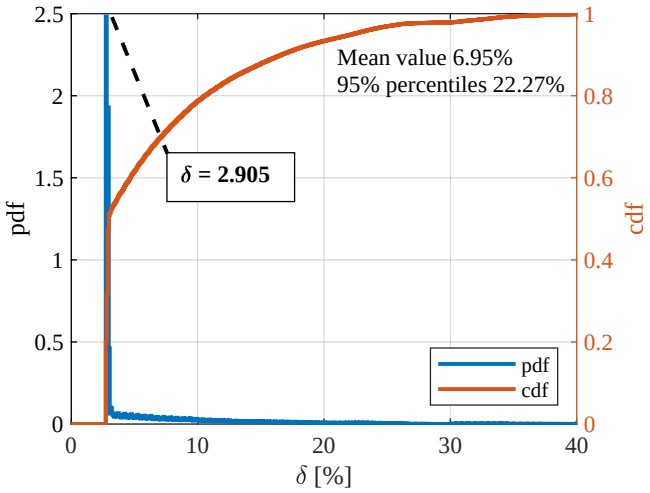


Fig. 13. Statistical analyses of the chopper duty cycle on the whole campaign.

metrologically characterize the rheostats positioned on-board the train, the resistance values were calculated from the voltage signals v_{F} and v_{HF} and from the current signals i_{RA} and i_{RB}.

The resistance R_B was obtained by making the ratio between v_{HF} and i_{RB}, for each single pulse, in correspondence to the current maximum value. The same is done for R_{A} considering i_{RA} and the voltage obtained as the difference $v_{\mathrm{F}} - v_{\mathrm{HF}}$.

When the GTO is turned on, a transient on the RL circuit starts. As long as the transient is not extinguished, there is a voltage drop across the stray inductance that reduces the current in the rheostats. Taking advantage of the very wide bandwidth of Rogowski coils, which do not give rise to overshoot when a current step occurs, it can be assumed that just after the peak current the transient is extinguished, therefore this current is a good estimation of $\hat{I}$, the steady state value for this pulse. Moreover the resistance value for this pulse can be calculated as the ratio between voltage and current in correspondence of this point. Another transient on the voltage occurs when the GTO reopens the RL circuit and the current is supplied by the inductance that closes the circuit on the flyback diode.

In order to clarify the explained procedure, Fig. 14 shows the development of v_{HF} and i_{RA} signals for a pulse in which the points used for the resistance measurement are marked with asterisks, $v_{\mathrm{R}}*$ and $\hat{I}_{\mathrm{RA}}$ for voltage and current respectively.

Note that the current may not reach its steady state value, in case of short duration pulses. To avoid this problem only pulses with a duty cycle greater than 5% were considered for the resistance estimation.

For each rheostat Fig.15 shows the PDF together with the mean value and the CoV (Coefficient of Variation, defined as the ratio between the standard deviation and the mean value). The classes on which the statistics are made are 100 and uniformly distributed, for values ranging from 1.52 Ω - 5% to 1.52 Ω + 5%.

The adoption of estimated mean value for R_{A} and R_{B} in the application of (8), greatly reduce the error on measurement of

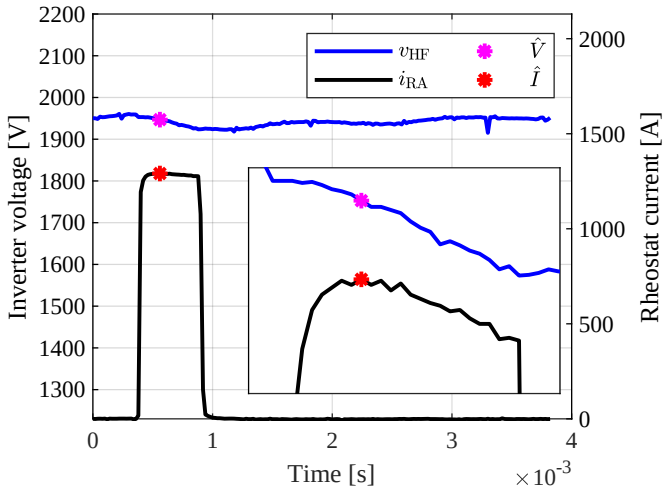


Fig. 14. Measurement points for the Resistance evaluation

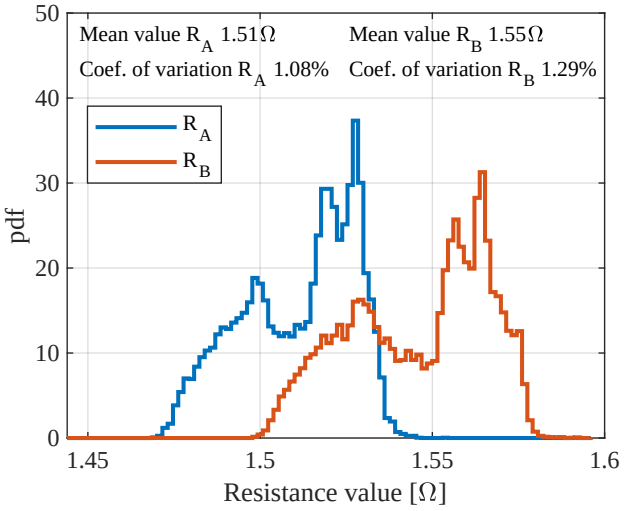


Fig. 15. Statistical analyses of the R_{A} and R_{B} values on the whole campaign

energy dissipated by the rheostats. The statistic shows how the values are concentrated in a very narrow range of occurrences, in particular the CoV is just over 1%, thus considerably less then the rated 5%. Therefore this greatly reduces the impact that resistance variation has on the performance of first method proposed (8). Of course on the second method there is no impact due to the variation of R_{A} and R_{B}, thanks to the estimation of $\hat{I}$.

VIII. Comparison with Reference Estimation System

In order to assess the metrological performances of the proposed methods, the wasted energy estimation has been compared with a reference estimation system already presented in the article [12].

According to [12], the reference energy for each pulse can be written as:

$$E_{\mathrm{REF}} = \sum_{\mathrm{k}=1}^{N} \frac{v_{\mathrm{INV}}[k] \cdot i_{\mathrm{R}}[k]}{fs} \cdot K_{\mathrm{DC}}(f(\delta_s)) * K_S(f(\delta_s)) \quad (16)$$

where:

- $v_{\mathrm{INV}}[k]$ is v_{F} for R_{A} and $(v_{\mathrm{F}} - v_{\mathrm{HF}})$ for R_{B};
- $i_{\mathrm{R}}[k]$ is $i_{\mathrm{RA}}[k]$ or $i_{\mathrm{RB}}[k]$;
- $K_{\mathrm{DC}}(\delta)$ is a correction coefficient that compensates for the error made by considering constant and the non-pulsed voltage across the rheostats;
- $K_S(\delta)$ is a correction coefficient to compensate for the transducer frequency response;
- $f(\delta_s)$ is the duty cycle estimated with (15);

The expanded relative uncertainty with a confidence level of 99% of the reference method is estimated as 0.20%.

The energy measured for each individual pulse using (8) and (11) can be compared to the E_{REF} trough:

$$\epsilon_1 = 100 \cdot \frac{E - E_{\mathrm{REF}}}{E_{\mathrm{REF}}}, \qquad \epsilon_2 = 100 \cdot \frac{\hat{E} - E_{\mathrm{REF}}}{E_{\mathrm{REF}}} \quad (17)$$

For the sake of brevity, only 2 out of 78 routes from the measurement campaign have been selected to show the performances of the two methods. On the route from Bussoleno to

Susa, there is only one braking arriving in Susa; Fig. 16 shows the results obtained on this braking. The percentage deviation ϵ_1 is depicted in blue, and ϵ_2 in red, calculated as (17) for each chopper pulse; moreover, the duty cycle estimated is reported in black. It can be seen that both methods perform very well in this braking: the deviations maintain limited to 1.48% for the first method and 0.86% for the second; evaluating the deviations on the total braking energy, ϵ_1 is 0.14% instead ϵ_2 is 0.12%; finally the standard deviation computed over all the pulses is 0.34% for ϵ_1 and only 0.14% for ϵ_2. The heating effect on the rheostat can be appreciated; in fact, the resistance increases during the braking, and, as a consequence, the ϵ_1 increases as well. As can be expected, the method (11) is independent of the variations of R, the error of the latter has a lower variability.

In order to analyze this temperature effect on a longer journey with multiple braking, Fig. 17 shows the results obtained on the route from Alessandria to Voghera. The two deviations (ϵ_1, ϵ_2) and the duty cycle (δ) are depicted with the same colors. Note that, obviously, the train is not in the braking stage for all the route, because the x-axis is not directly the time. Those three quantities are plotted versus the pulses, for this reason, only the braking are reported, one after the other. On this route, it is possible to see what happens during high dissipative braking, the duty cycle is greater than 30% multiple times. From the chart is evident that an increase in the duty cycle is followed, with some delay, by an increment in ϵ_1. The delay is due to the thermal transient of the braking rheostat. In the monitored locomotive, the resistance has a variability of 1.08 %, which includes the thermal effect, already shown in Fig. 15. In fact, the standard deviation of results obtained on pulses is 0.70%, moreover the error on the total braking energy is 0.69%.

As regards the second method, the performances are better (maximum error on a single current pulse is slightly over 1%, the standard deviation is 0.33%); nevertheless, for more dissipative braking ($\delta > 30\%$), ϵ_1 increases proportionally to duty. This is due to the fact that the current i_{RA} is not constant during the single pulse, as it can be noted from Fig. 14. More in detail i_{RA} decreases as the filter capacitance is discharging (v_{HF} decreases). Moreover, the current decreases also because the rheostat is heated by Joule effect (thus, the resistance is increasing). During the pulse with a big duty cycle, the estimation made with $\hat{I}$ has a worst accuracy, but considering the statistical distribution of Fig. 13, it can be concluded that this condition is unlikely to occur, thus it has little impact on average error.

IX. Conclusion

Measuring energy in presence of chopped waveforms is a challenging task as that in the braking resistors for railway applications, but it is useful to quantify the amount of energy that could be recovered. In this article a new approach to simplify this task is proposed and applied to real test cases coming from measurement campaign on-board train. It is easy to implement because it relies only on information already available to the train control unit. Despite its simplicity, it allows taking into account the current transient due to the presence of the rheostat inductance. It allows obtaining fairly accurate results (1%). It is possible to enhance the performance of the method by installing a current peak detector to overcome the issue of resistance variation with temperature. Still maintaining the cost low, it allows for reaching accuracies comparable with the reference method, its average deviation on the energy measurement is 0.46%.

Funding

This research was funded by the EMPIR program co-financed by the participating countries and the European Union's Horizons 2020 research and innovation program, project name MyRailS, grant number 16ENG04.

Acknowledgment

The authors wish to thank Trenitalia for the support during the measurement campaign.

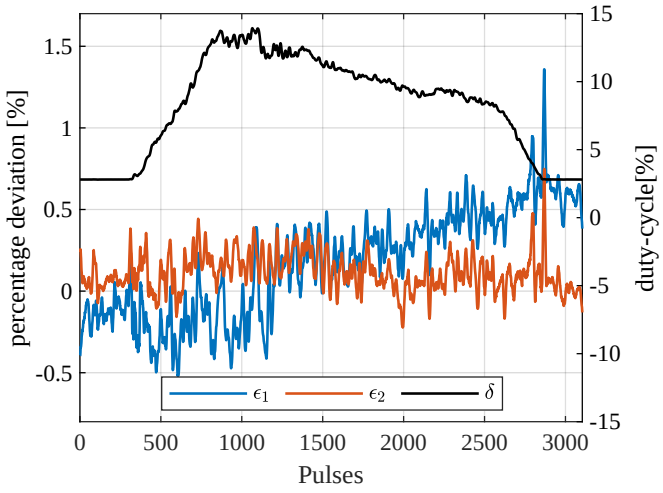


Fig. 16. Application to the railway journey from Bussoleno to Susa

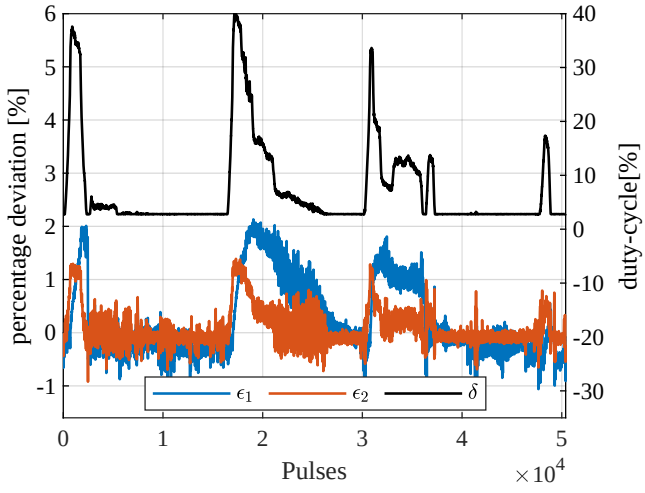


Fig. 17. Application to the railway journey from Alessandria to Voghera

REFERENCES

[1] E. Commission. (2011, Mar.) White paper roadmap to a single european transport area – towards a competitive and resource efficient transport system /* com/2011/0144 final */. [Online]. Available: eur-lex.europa.eu/legal-content/EN/ALL/?uri=CELEX:52011DC0144

[2] M. Brenna, F. Foiadelli, and D. Zaninelli, *Electrical railway transportation systems*. John Wiley & Sons, 2018.

[3] L. Liudvinavičius and L. Lingaitis, "Electrodynamic braking in high-speed rail transport," *Transport*, vol. 22, 07 2007.

[4] D. Ramsey, T. Letrouve, A. Bouscayrol, and P. Delarue, "Comparison of energy recovery solutions on a suburban dc railway system," *IEEE Transactions on Transportation Electrification*, pp. 1–1, 2020.

[5] M. Popescu and A. Bitoleanu, "A review of the energy efficiency improvement in dc railway systems," *Energies*, vol. 12, no. 6, 2019.

[6] C. Wu, S. Lu, F. Xue, L. Jiang, and M. Chen, "Optimal sizing of onboard energy storage devices for electrified railway systems," *IEEE Transactions on Transportation Electrification*, vol. 6, no. 3, pp. 1301–1311, 2020.

[7] G. Cipolletta, A. Delle Femine, D. Gallo, M. Luiso, and C. Landi, "Design of a stationary energy recovery system in rail transport," *Energies*, vol. 14, no. 9, 2021.

[8] M. Dominguez, A. Fernández-Cardador, A. P. Cucala, and R. R. Pecharroman, "Energy savings in metropolitan railway substations through regenerative energy recovery and optimal design of ato speed profiles," *IEEE Transactions on Automation Science and Engineering*, vol. 9, no. 3, pp. 496–504, 2012.

[9] S. Su, X. Wang, Y. Cao, and J. Yin, "An energy-efficient train operation approach by integrating the metro timetabling and eco-driving," *IEEE Transactions on Intelligent Transportation Systems*, vol. 21, no. 10, pp. 4252–4268, 2020.

[10] F. Cascetta, G. Cipolletta, A. Delle Femine, J. Quintana Fernández, D. Gallo, D. Giordano, and D. Signorino, "Impact of a reversible substation on energy recovery experienced on-board a train," *Measurement*, p. 109793, 2021.

[11] J. Lehr and P. Ron, *Pulsed Voltage and Current Measurements*, 2018, pp. 493–546.

[12] D. Giordano, D. Signorino, D. Gallo, H. E. van den Brom, and M. Sira, "Methodology for the accurate measurement of the power dissipated by braking rheostats," *Sensors*, vol. 20, no. 23, 2020. [Online]. Available: https://www.mdpi.com/1424-8220/20/23/6935

[13] EURAMET, "Metrology for smart energy management in electric railway systems," 16ENG04 MyRailS, 2017.

[14] A. Delle Femine, D. Gallo, D. Giordano, C. Landi, M. Luiso, and D. Signorino, "Power quality assessment in railway traction supply systems," *IEEE Transactions on Instrumentation and Measurement*, vol. 69, no. 5, pp. 2355–2366, 2020.

[15] "Railway applications - Supply voltages of traction systems ," CEI-CT9, CEI-SC9C, Standard, 2006.

[16] A. Delle Femine, D. Gallo, C. Landi, and M. Luiso, "Discussion on dc and ac power quality assessment in railway traction supply systems," vol. 2019-May, 2019.

[17] M. Norgia, A. Pesatori, and A. Colombo, "Temperature measurement system for train rheostat," in *2013 IEEE International Instrumentation and Measurement Technology Conference (I2MTC)*, 2013, pp. 484–487.

[18] G. Crotti, D. Giordano, D. Signorino, A. Delle Femine, D. Gallo, C. Landi, M. Luiso, A. Biancucci, and L. Donadio, "Monitoring energy and power quality on board train," in *2019 IEEE 10th International Workshop on Applied Measurements for Power Systems (AMPS)*, 2019, pp. 1–6.

[19] I. O. for Standardization, *Guide to the expression of uncertainty in measurement, Supported by BIPM, IEC, IFCC, ISO IUPAC, IUPAP and OIML*, Geneva, 2008.

[20] G. Crotti, A. Delle Femine, D. Gallo, D. Giordano, C. Landi, and M. Luiso, "Calibration of voltage and current transducers for dc railway systems," *IEEE Transactions on Instrumentation and Measurement*, vol. 68, no. 10, pp. 3850–3860, 2019.

[21] I. O. for Standardization, *Guide to the expression of uncertainty in measurement (GUM)-Supplement 1: Numerical methods for the propagation of distributions*, Geneva, 2004.